



Article

# The Influence Mechanism of Neutron Kinetics of the Accelerator-Driven Subcritical Reactor Based on the Fast/Thermal Neutron Spectra by Monte Carlo Homogenization Method

Nianbiao Deng <sup>1</sup>, Chao Xie <sup>2</sup>, Cheng Hou <sup>3</sup>, Zhulun Li <sup>4</sup>, Jinsen Xie <sup>2,\*</sup> and Tao Yu <sup>2,\*</sup><sup>1</sup> School of Resource Environment and Safety Engineering, University of South China, Hengyang 421001, China<sup>2</sup> School of Nuclear Science and Technology, University of South China, Hengyang 421001, China<sup>3</sup> China Institute of Atomic Energy, Beijing 102413, China<sup>4</sup> School of Nuclear Science and Engineering, North China Electric Power University, Beijing 102206, China

\* Correspondence: jinsen\_xie@usc.edu.cn (J.X.); yutao29@sina.com (T.Y.)

**Abstract:** For the sake of understanding the mechanism of deep subcriticality and high heterogeneity of neutron fluence rate in time–space on the neutron kinetics of the Accelerator-driven Subcritical Reactor (ADSR) under varied beam transients and neutron spectra. A Monte Carlo homogenization approach for the neutron time–space kinetics of the ADSR is proposed in this study, and the influence mechanism on the kinetic parameters of the ADSR under varied neutron spectra, subcriticality, and beam transients is examined. The results show that the Monte Carlo homogenization for the  $\alpha$  eigenvalue mode is more adaptable to the subcriticality characteristics under varied subcriticality; under beam transients, the relative differences in the kinetic parameters of the different modes of the ADSR with fast/thermal spectra increase with the depth of subcriticality, and the differences in neutron generation time for varied modes are larger than those of effective fraction of delayed neutron. Thus, it is recommended to use a more adaptable Monte Carlo homogenization method for the time–space kinetics of ADSR, and the effects of the high heterogeneity of neutron fluence rate and deep subcriticality in time–space on the neutron generation time should be considered.

**Keywords:** Monte Carlo homogenization method; ADS Subcritical Reactor; neutron kinetics; deep subcriticality; heterogeneity of neutron fluence rate in time–space



**Citation:** Deng, N.; Xie, C.; Hou, C.; Li, Z.; Xie, J.; Yu, T. The Influence Mechanism of Neutron Kinetics of the Accelerator-Driven Subcritical Reactor Based on the Fast/Thermal Neutron Spectra by Monte Carlo Homogenization Method. *Energies* **2023**, *16*, 3545. <https://doi.org/10.3390/en16083545>

Academic Editor: Oleg Leonidovich Tashlykov

Received: 22 March 2023

Revised: 6 April 2023

Accepted: 18 April 2023

Published: 19 April 2023



**Copyright:** © 2023 by the authors. Licensee MDPI, Basel, Switzerland. This article is an open access article distributed under the terms and conditions of the Creative Commons Attribution (CC BY) license (<https://creativecommons.org/licenses/by/4.0/>).

## 1. Introduction

The future trend of international electricity consumption is a continuous increase in the total amount, and the development of clean energy is a strategic choice for sustainable global energy development. Nuclear energy, as an important clean and low-carbon energy source, has the advantages of continuous and stable power output as well as the ability to release large amounts of electricity from a very small number of resources [1,2]. The safe treatment and disposal of spent fuel, especially the long-lived highly radioactive nuclear waste, will become one of the bottlenecks affecting the sustainable development of nuclear energy [3]. An accelerator-driven subcritical system (ADS) is a powerful tool to solve the spent-fuel problem and to achieve transmutation, and it can also be used as an efficient nuclear fuel breeding device due to its high neutron redundancy [4,5]. Therefore, the development of ADS technology is a feasible route to ensure energy security and achieve the sustainable development of nuclear energy.

To completely understand the kinetic aspects of operation and guarantee the dependability of management and security systems, ADSR neutron kinetics must be investigated [6,7]. When compared to the critical reactor system, the subcritical ADSR has

dozens of unique neutronic properties, the most notable of which is that the neutron kinetic behavior of the ADSR differs significantly from that of the critical state due to the addition of an external neutron source and the core's subcriticality [8]. ADSR neutron kinetics are distinguished by deep subcriticality and the high heterogeneity of the neutron fluence rate in time–space.

Solving neutron kinetics processes in the study of ADSR neutron kinetics issues is mainly based on the computationally efficient deterministic method [8]. The deterministic method calculation is usually divided into two steps based on the generation of homogenized group constants and the calculation of core deterministic neutron diffusion/transport. It is very significant for the study of neutron kinetics in an ADSR, namely, how to obtain accurate homogenized group constants so that the results of the core homogenization calculations are consistent with those of the non-homogenized ones [9,10].

Several studies are currently being conducted both nationally and internationally to investigate the homogenized group constants for the neutron kinetics of an ADSR [8,11–14]. The majority of existing research only takes into account a single steady-state mode condition, not beam transients. The existing homogenized group constants do not accurately reflect the ADSR properties during beam transients [15,16].

The homogenized group constants in different modes are proposed to address the issue that the existing single homogenized group constants are not accurate for the neutron fluence rate under beam transients [17]. Using the self-developed deterministic code TRIONES, the authors built multi-mode core few-group constants that are more adaptive to neutron kinetics, and they investigated the relevant kinetic features for an ADSR [18–20].

Due to the obvious advantages of the Monte Carlo (referred to as MC) method's continuous energy compared with deterministic methods, such as its powerful geometric processing capability and no need for problem-specific resonance calculations [21], the accurate simulation of an ADSR with high heterogeneity in time–space can be effectively solved. However, if the MC method is used throughout, its computational efficiency is too low for a large number of core schemes [22]. In order to maximize computing efficiency, the homogenized group constants derived by the MC approach are provided to the following deterministic neutron dynamics core software in this article.

The traditional MC homogenization methods only consider the fundamental neutron fluence rate, which cannot accurately describe the deep subcriticality and high heterogeneity of the neutron fluence rate in time–space of the ADSR under beam transients. Therefore, in order to accurately describe the characteristics of an ADSR under beam transients, different modes of MC homogenization methods can be considered for different beam transients, and a set of MC homogenization methods for the neutron time–space kinetics for an ADSR can be developed.

The neutron energy spectrum is crucial for the study of neutron kinetics in an ADSR, and there are few comparative studies on the kinetic properties of an ADSR for different classes of neutron energy spectra, such as the fast neutron spectrum (referred to as fast spectrum) and thermal neutron spectrum (referred to as thermal spectrum).

Thus, for the sake of overcoming the shortcomings of the existing studies, the deep subcriticality and high heterogeneity of the neutron fluence rate in time–space for an ADSR are accurately described. In this paper, we firstly carry out the study of the  $\lambda$  eigenvalue mode (referred to as  $\lambda$  mode) MC homogenization method and verify the ADSR benchmark; secondly, we carry out the study of the  $\alpha$  eigenvalue mode (referred to as  $\alpha$  mode) MC homogenization method based on the improved  $\alpha$ -k iterative method and verify the ADSR benchmark; finally, for ADSR with fast and thermal spectra, the mechanism of each mode kinetic parameter of an ADSR during beam transients is examined.

The MC homogenization method for ADSR neutron kinetics will be developed to reveal the mechanism of ADSR time–space neutron kinetics under different neutron spectra, subcriticalities, and beam transient conditions. The advancement of this study is critical for refining the theory of neutron kinetics in an ADSR.

The remainder of the paper is structured as follows. The calculation tool and model are described in Section 2. In Section 3, we present a method for ADSR time–space neutron kinetics using MC homogenization. Section 4 presents a study of the ADSR time–space neutron kinetics influence mechanism with different neutron spectra. Section 5 finally discusses our conclusions.

## 2. Computational Tool and Model

### 2.1. Calculation and Analysis Tools

The research on the MC homogenization method will be carried out based on the open-source program OpenMC [23], where the study of the  $\lambda$ -mode MC homogenization method is carried out (version 0.12.1). The study of the  $\alpha$ -mode MC homogenization method is carried out using the self-developed OpenMC-PA program. This program is based on the open-source program OpenMC, and the OpenMC-PA program with  $\alpha$  eigenvalue calculation has been developed based on the improved  $\alpha$ -k iterative method [24,25], and all its related functions have been verified [26].

The self-developed TRIONES software, which can compute the fluctuation of neutron fluence rate and kinetic parameters with time and space for the  $\lambda/\alpha$  mode of the core, has been used to study the mechanism of time–space neutron kinetics in an ADSR. The relevant functions of the TRIONES program have been verified [18].

### 2.2. Calculation Model

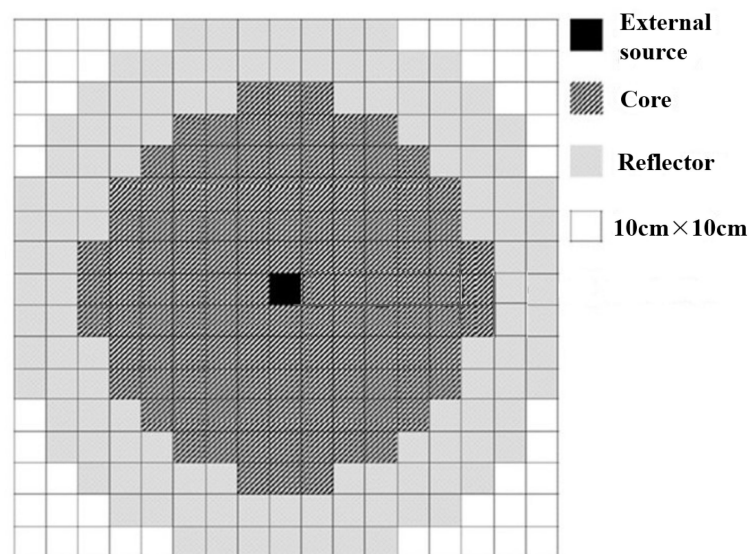
In this paper, we will use the ADSR benchmark designed by OpenMC. The ADSR geometry reference [27] is shown in Figure 1. The fuel and reflector layers have been defined as a grid of  $10 \times 10 \times 10 \text{ cm}^3$  with 17, 17, and 16 layers in the X, Y, and Z directions, respectively [28]. The fuel is considered to be MOX fuel mixed with  $\text{UO}_2$  and  $^{239}\text{PuO}_2$ . The reflector for the ADSR in the fast spectrum is chosen to be a natural Fe material, and the reflector in the thermal spectrum is chosen to be a light water material containing boron. The kinetic characteristics at different subcriticalities are studied by calculating the three typical core loading schemes by OpenMC with  $k_{\text{eff}} = 0.99, 0.97,$  and  $0.95$  by adjusting the  $^{239}\text{PuO}_2$  content in MOX fuel. Tables 1 and 2 show the core material compositions of the fast/thermal spectra for the three core loading schemes.

**Table 1.** ADSR material composition with fast spectrum for three core loading schemes.

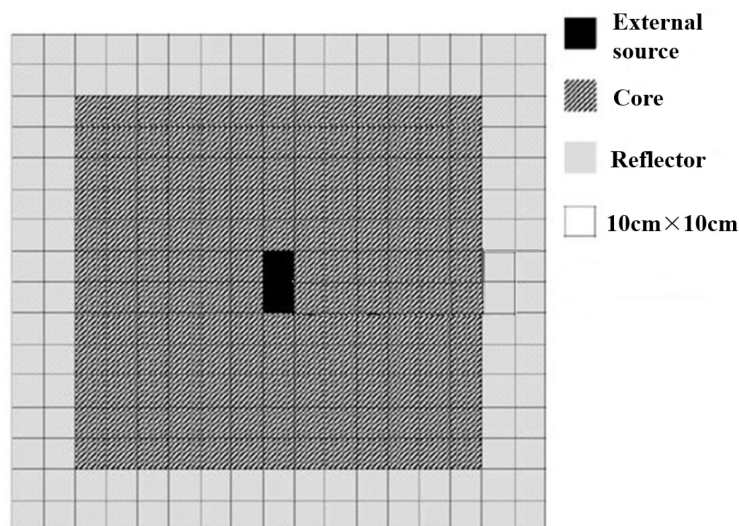
| $k_{\text{eff}}$ | Material Composition of Fuel (Nuclide Density $10^{24}/\text{cm}^3$ )                                                                                   | Material Composition of Reflector (Nuclide Density $10^{24}/\text{cm}^3$ )     |
|------------------|---------------------------------------------------------------------------------------------------------------------------------------------------------|--------------------------------------------------------------------------------|
| 0.99             | $^{16}\text{O} 6.667 \times 10^{-1}$ $^{235}\text{U} 9.477 \times 10^{-3}$ $^{238}\text{U} 3.064 \times 10^{-1}$ $^{239}\text{Pu} 1.744 \times 10^{-2}$ | $^{54}\text{Fe} 2.708 \times 10^{-3}$<br>$^{56}\text{Fe} 4.210 \times 10^{-2}$ |
| 0.97             | $^{16}\text{O} 6.667 \times 10^{-1}$ $^{235}\text{U} 9.507 \times 10^{-3}$ $^{238}\text{U} 3.074 \times 10^{-1}$ $^{239}\text{Pu} 1.644 \times 10^{-2}$ | $^{57}\text{Fe} 9.638 \times 10^{-4}$                                          |
| 0.95             | $^{16}\text{O} 6.667 \times 10^{-1}$ $^{235}\text{U} 9.536 \times 10^{-3}$ $^{238}\text{U} 3.083 \times 10^{-1}$ $^{239}\text{Pu} 1.546 \times 10^{-2}$ | $^{58}\text{Fe} 1.285 \times 10^{-4}$                                          |

**Table 2.** ADSR material composition with thermal spectrum for three core loading schemes.

| $k_{\text{eff}}$ | Material Composition of Fuel (Nuclide Density $10^{24}/\text{cm}^3$ )                                                                                   | Material Composition of Reflector (Nuclide Density $10^{24}/\text{cm}^3$ ) |
|------------------|---------------------------------------------------------------------------------------------------------------------------------------------------------|----------------------------------------------------------------------------|
| 0.99             | $^{16}\text{O} 6.667 \times 10^{-1}$ $^{235}\text{U} 9.492 \times 10^{-3}$ $^{238}\text{U} 3.069 \times 10^{-1}$ $^{239}\text{Pu} 1.694 \times 10^{-2}$ | $^1\text{H} 4.946 \times 10^{-2}$<br>$^{16}\text{O} 2.467 \times 10^{-2}$  |
| 0.97             | $^{16}\text{O} 6.667 \times 10^{-1}$ $^{235}\text{U} 9.522 \times 10^{-3}$ $^{238}\text{U} 3.079 \times 10^{-1}$ $^{239}\text{Pu} 1.594 \times 10^{-2}$ | $^{10}\text{B} 8.200 \times 10^{-6}$                                       |
| 0.95             | $^{16}\text{O} 6.667 \times 10^{-1}$ $^{235}\text{U} 9.554 \times 10^{-3}$ $^{238}\text{U} 3.089 \times 10^{-1}$ $^{239}\text{Pu} 1.488 \times 10^{-2}$ | $^{11}\text{B} 3.222 \times 10^{-5}$                                       |



(a) Horizontal profile



(b) Vertical profile

**Figure 1.** ADSR schematic diagram.

### 3. Monte Carlo Homogenization Method for ADSR Time–Space Neutron Kinetics

#### 3.1. Method Overview

For the MC homogenization method, the method of volume flux weights is used to obtain the homogenized group constants of the calculated objects. In this paper, the collision probability method is used to calculate the group transfer probability and the higher-order scattering matrix when performing the transport correction for the anisotropic scattering effect, thus reducing the error introduced by the two-stage method in calculating the transport correction. Nevertheless, because of the large statistical uncertainty and poor computational efficiency [22] of the higher-order scattering-moment matrix, the third-order scattering-moment matrix is used for the anisotropic scattering cross-section.

In order to accurately describe the characteristics in an ADSR under beam transients, different modes of the MC homogenization method will be considered for different beam transient operating conditions. The  $\lambda$ -mode MC homogenization method, which considers the most commonly used  $\lambda$  eigenvalue in the traditional neutron kinetics analysis. The  $\alpha$ -mode MC homogenization method is studied with the  $\alpha$  eigenvalue used for its consideration. By linking the library of  $\lambda$ -mode and  $\alpha$ -mode MC-homogenized group

constants generated by the above two modes, and adapting them to the beam transient conditions, a set of MC homogenization method for ADSR time-space neutron kinetics can be constructed.

Based on the deterministic two-stage method, ADSR-homogenized group constants for the  $\lambda/\alpha$  mode generated by the MC homogenization method are applied to the TRIONES program for the  $\lambda/\alpha$  mode, respectively. The study on the mechanism of ADSR time-space neutron kinetics with different neutron spectra under beam transients is carried out. Figure 2 depicts the flow chart of the entire computation technique.

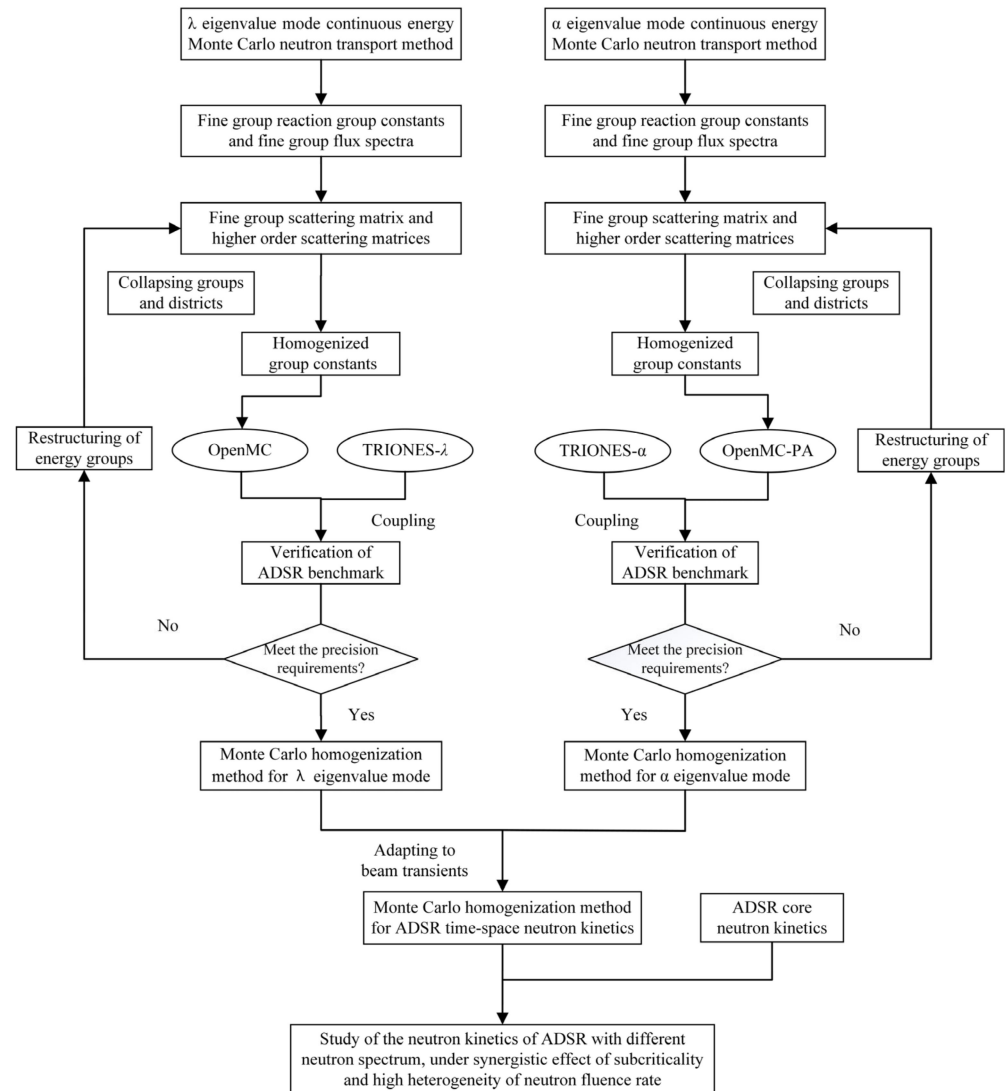


**Figure 2.** Flow chart of the entire calculation method.

### 3.2. Energy Group Division

The energy spectra of the fast/thermal spectra in ADSR at typical subcriticality  $k_{\text{eff}} = 0.97$  are given in Figures 3 and 4, respectively. The flux given in Figures 3 and 4 are the normalized neutron flux density.

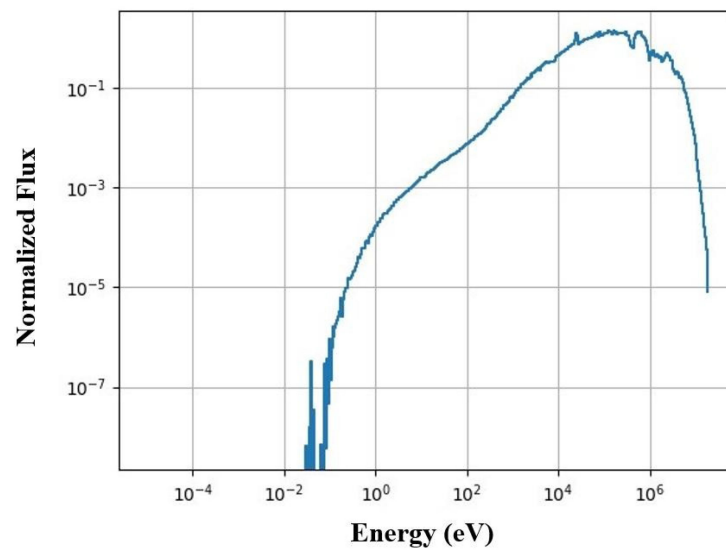


Figure 3. Energy spectra diagram of ADSR of fast spectrum ( $k_{\text{eff}} = 0.97$ ).

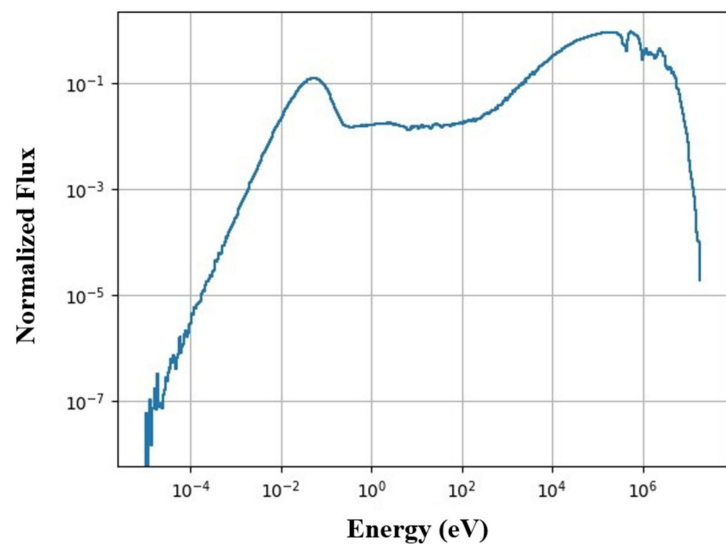


Figure 4. Energy spectra diagram of ADSR of thermal spectrum ( $k_{\text{eff}} = 0.97$ ).

For the energy group division of the fast spectrum in ADSR, referring to the typical energy group structure of fast reactor ERAONS 33 group structure [29] and the suggestions of the literature [8], as well as combining its energy spectrum characteristics (Figure 3) and calculation efficiency, after a large number of verification schemes, the calculation of the homogenized group constants of the fast spectrum finally considers the 12-group energy group structure. For the thermal spectrum of the ADSR, after considering the energy spectrum characteristics (Figure 4) and the calculation accuracy and efficiency, the eight-group energy group structure is finally considered for the calculation of the thermal spectrum. The energy group division of the fast/thermal neutron spectra is shown in Table 3.

**Table 3.** Energy group division of the fast/thermal spectra.

| Energy Group Number | Energy Group Upper Boundary (MeV) |                            |
|---------------------|-----------------------------------|----------------------------|
|                     | 12-Group (Fast Spectrum)          | 8-Group (Thermal Spectrum) |
| 1                   | $1.9640 \times 10^1$              | $1.9640 \times 10^1$       |
| 2                   | 6.6053                            | $8.2100 \times 10^{-1}$    |
| 3                   | 2.2313                            | $2.4788 \times 10^{-2}$    |
| 4                   | $8.2085 \times 10^{-1}$           | $2.0347 \times 10^{-3}$    |
| 5                   | $4.9787 \times 10^{-1}$           | $4.5400 \times 10^{-4}$    |
| 6                   | $1.8316 \times 10^{-1}$           | $2.2603 \times 10^{-5}$    |
| 7                   | $6.7380 \times 10^{-2}$           | $4.0000 \times 10^{-6}$    |
| 8                   | $2.4788 \times 10^{-2}$           | $5.4000 \times 10^{-7}$    |
| 9                   | $9.1182 \times 10^{-3}$           |                            |
| 10                  | $2.0347 \times 10^{-3}$           |                            |
| 11                  | $4.5400 \times 10^{-4}$           |                            |
| 12                  | $4.0000 \times 10^{-6}$           |                            |

### 3.3. The Monte Carlo Homogenization Method for the $\lambda$ Eigenvalue Mode

The heterogeneous transport criticality calculation for the ADSR is performed using the OpenMC to obtain the accurate values of the three  $k_{\text{eff}}$ , based on the continuous-energy MC calculation. Additionally, it is used as the reference value to verify the homogenized group constants. The homogenized group constants for each ADSR material are calculated using the energy group division given in Table 3 and the  $\lambda$ -mode MC homogenization method described in Section 3.1. Then, it is applied to the core diffusion program TRIONES- $\lambda$  for the  $\lambda$  mode to obtain the core  $k_{\text{eff}}$  and verify the accuracy of the corresponding group constants.

The results of the verification of the homogenized group constants for the fast/thermal spectra of the ADSR in the  $\lambda$  mode are shown in Table 4. From the results in Table 4, it can be seen that the computational accuracy of the homogenized group constants for the  $\lambda$  mode generated by the ADSR fast/thermal neutron spectra all meet the requirements.

**Table 4.** The results of the verification of the homogenized group constants for the fast/thermal spectra of the ADSR in the  $\lambda$  mode.

| Type of Energy Spectrum | $k_{\text{eff}}$ | $k_{\text{eff}}$ of Continuous-Energy MC for the $\lambda$ Mode (Reference Value) | $k_{\text{eff}}$ of TRIONES- $\lambda$ | Relative Error |
|-------------------------|------------------|-----------------------------------------------------------------------------------|----------------------------------------|----------------|
| Fast spectrum           | 0.99             | 0.99086                                                                           | 0.99273                                | 188 pcm        |
|                         | 0.97             | 0.97044                                                                           | 0.96904                                | −144 pcm       |
|                         | 0.95             | 0.95003                                                                           | 0.95199                                | 207 pcm        |
| Thermal spectrum        | 0.99             | 0.99053                                                                           | 0.98885                                | −169 pcm       |
|                         | 0.97             | 0.97078                                                                           | 0.96955                                | −127 pcm       |
|                         | 0.95             | 0.94971                                                                           | 0.94912                                | −62 pcm        |

### 3.4. The Monte Carlo Homogenization Method for the $\alpha$ Eigenvalue Mode

The heterogeneous transport criticality calculation for the ADSR is performed using the OpenMC-PA to obtain the accurate values of the three  $k_{\text{eff}}$ , based on the continuous-energy MC calculation. Additionally, it is used as the reference value to verify the homogenized group constants. The homogenized group constants for each ADSR material are calculated using the  $\alpha$ -mode MC homogenization method described in Section 3.1. Then, it is applied to the core diffusion program TRIONES- $\alpha$  for the  $\alpha$  mode to obtain the core  $k_{\text{eff}}$  and verify the accuracy of the corresponding group constants. The energy group division of the fast/thermal spectra of the  $\alpha$  mode is also adopted in Table 3.

The results of the verification of the homogenized group constants for the fast/thermal spectra of the ADSR in the  $\alpha$  mode are shown in Table 5. From the results in Table 5, it can be seen that the computational accuracy of the homogenized group constants for the  $\alpha$  mode generated by the ADSR fast/thermal spectra all meet the requirements.

**Table 5.** The results of the verification of the homogenized group constants for the fast/thermal spectra of the ADSR in the  $\alpha$  mode.

| Type of Energy Spectrum | $k_{\text{eff}}$ | $k_{\text{eff}}$ of Continuous-Energy MC for the $\alpha$ Mode (Reference Value) | $k_{\text{eff}}$ of TRIONES- $\alpha$ | Relative Error |
|-------------------------|------------------|----------------------------------------------------------------------------------|---------------------------------------|----------------|
| Fast spectrum           | 0.99             | 0.99073                                                                          | 0.99179                               | 107 pcm        |
|                         | 0.97             | 0.97051                                                                          | 0.97166                               | −119 pcm       |
|                         | 0.95             | 0.94995                                                                          | 0.94832                               | −172 pcm       |
| Thermal spectrum        | 0.99             | 0.99013                                                                          | 0.98867                               | −148 pcm       |
|                         | 0.97             | 0.97085                                                                          | 0.97134                               | 50.7 pcm       |
|                         | 0.95             | 0.94921                                                                          | 0.95000                               | 83.2 pcm       |

When the results in Tables 4 and 5 are compared, it is clear that the calculation accuracy of the  $\alpha$ -mode MC homogenization method is generally higher than that of the mode MC homogenization method at various subcriticalities. That is, the  $\alpha$ -mode MC homogenization method is more adaptable to the subcriticality property. The physical mechanism is that the  $\alpha$  eigenvalue is the “natural eigenvalue” for describing the neutron breeding characteristics of the off-critical reactor, which is advantageous for describing the time evolution of the neutron kinetics of the ADSR.

#### 4. Study of the Influence Mechanism of the ADSR Time–Space Neutron Kinetics with Different Neutron Spectra

The influence of subcriticality and external source on the kinetic parameters of an ADSR with varied neutron spectrums during beam transients will be investigated. In this section, the kinetic parameters are investigated in the  $\lambda$  and  $\alpha$  modes for an ADSR with different neutron spectra under beam transients. The beam trip and the starting process are the two types of beam transient conditions considered. The study of kinetic parameters mainly considers neutron generation time  $\Lambda$  and the effective fraction of the delayed neutron  $\beta_{\text{eff}}$ . For both beam transient situations, the time step is  $1.0 \times 10^{-5}$  s and the simulation time is  $3 \times 10^{-3}$  s.

##### 4.1. Study of the Mechanism of ADSR Kinetic Parameters on the Fast Spectrum

This section describes the influence mechanism of the ADSR kinetic parameters for the fast spectrum, starting with the study of  $\Lambda$ . The relative differences in  $\Lambda$  with time for the  $\lambda$  and  $\alpha$  modes are shown in Figures 5 and 6 for the beam trip and starting process, respectively.

We can see from Figure 5 that under the beam trip scenario the relative difference  $\Lambda$  between both the modes fluctuates at the outset and becomes smooth as the time increases. Figure 6 shows that the relative  $\Lambda$  differences between two modes fluctuates greatly at the beginning of starting process and smooths out with the increase in time. In both cases, the relative difference  $\Lambda$  between both the modes increases with the deepening of the subcriticality.

The relative differences in  $\beta_{\text{eff}}$  with time for the  $\lambda$  and  $\alpha$  modes are shown in Figures 7 and 8 for the beam trip and starting process, respectively.

From Figure 7, the relative differences in  $\beta_{\text{eff}}$  between the two modes tend to be smooth under beam trip and increase with the deepening of the subcriticality. Figure 8 shows that the relative differences in  $\beta_{\text{eff}}$  between both the modes tend to be smooth under the starting process, increasing with the deepening of the subcriticality.



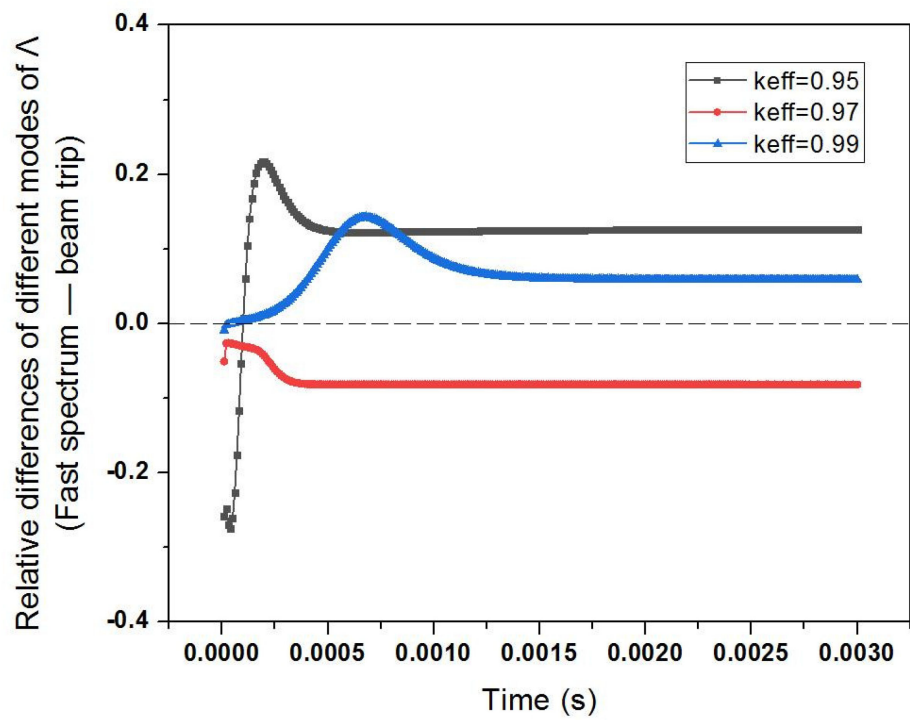


Figure 5. Relative differences in  $\Lambda$  with time for different modes of the fast spectrum, under different subcriticalities and beam trips.

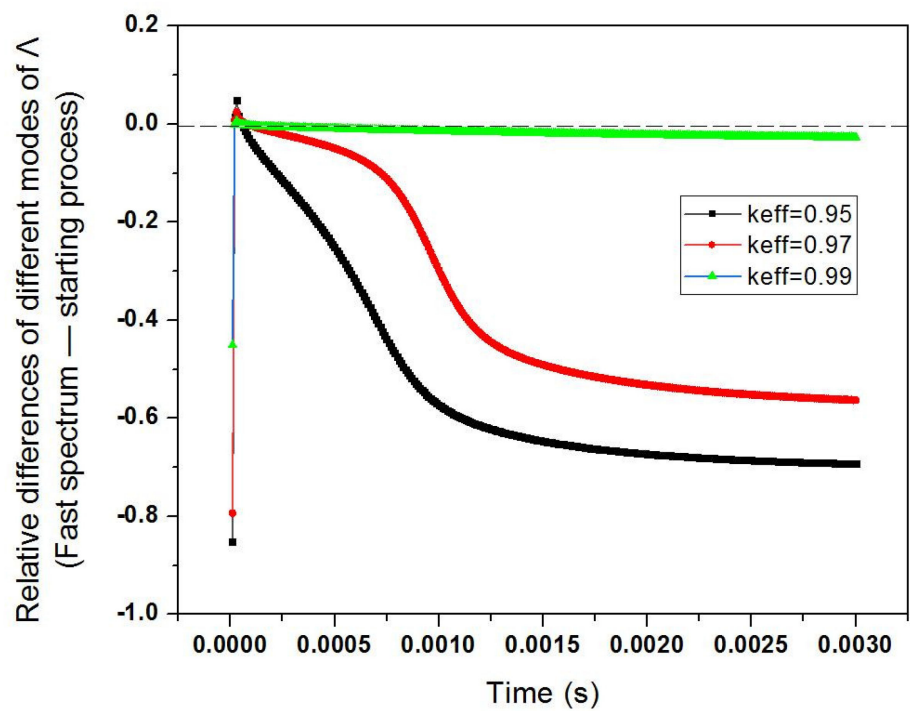
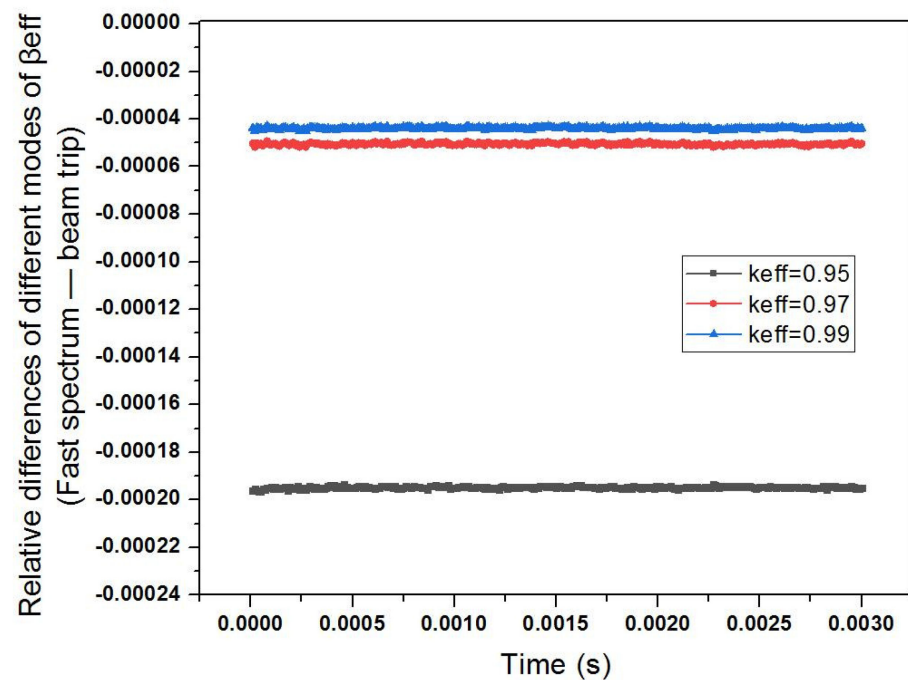
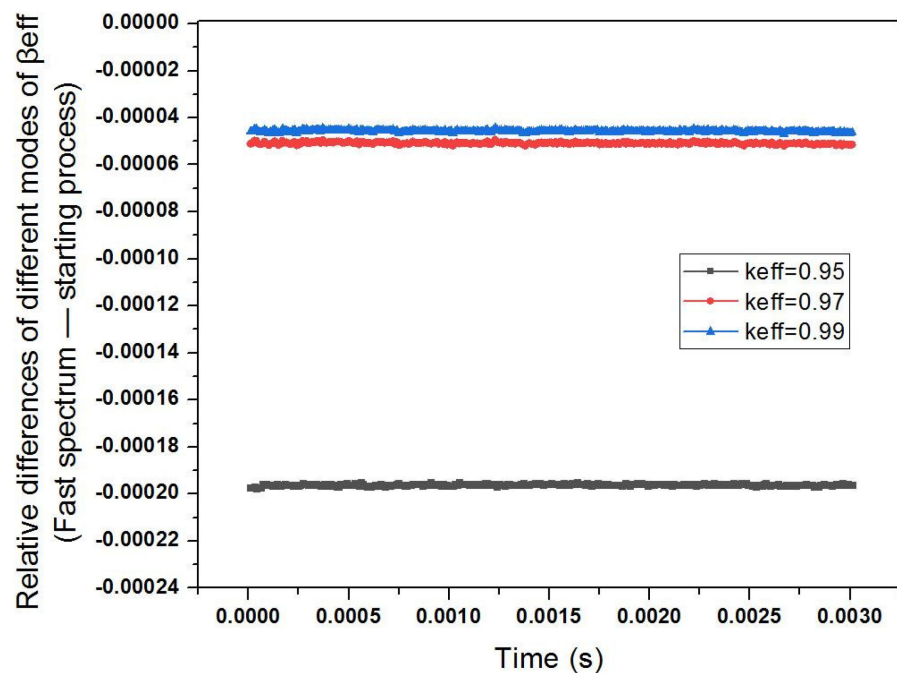


Figure 6. Relative differences in  $\Lambda$  with time for different modes of the fast spectrum, under different subcriticalities and starting processes.



**Figure 7.** Relative differences in  $\beta_{\text{eff}}$  with time for different modes of the fast spectrum, under different subcriticalities and beam trips.



**Figure 8.** Relative differences in  $\beta_{\text{eff}}$  with time for different modes of the fast spectrum, under different subcriticalities and starting processes.

#### 4.2. Study of the Mechanism of ADSR Kinetic Parameters on the Thermal Spectrum

In this section, we study the influence mechanism of the ADSR kinetic parameters for the thermal spectrum, starting with the study of  $\Lambda$ . The relative differences in  $\Lambda$  with time for the  $\lambda$  and  $\alpha$  modes are shown in Figures 9 and 10 for the beam trip and starting process, respectively.

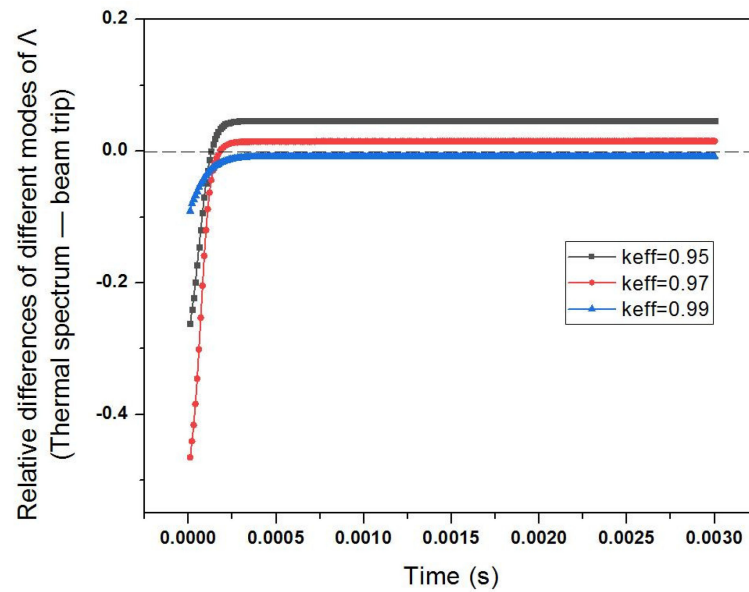


**Figure 9.** Relative differences in  $\Lambda$  with time for different modes of the thermal spectrum, under different subcriticalities and beam trips.

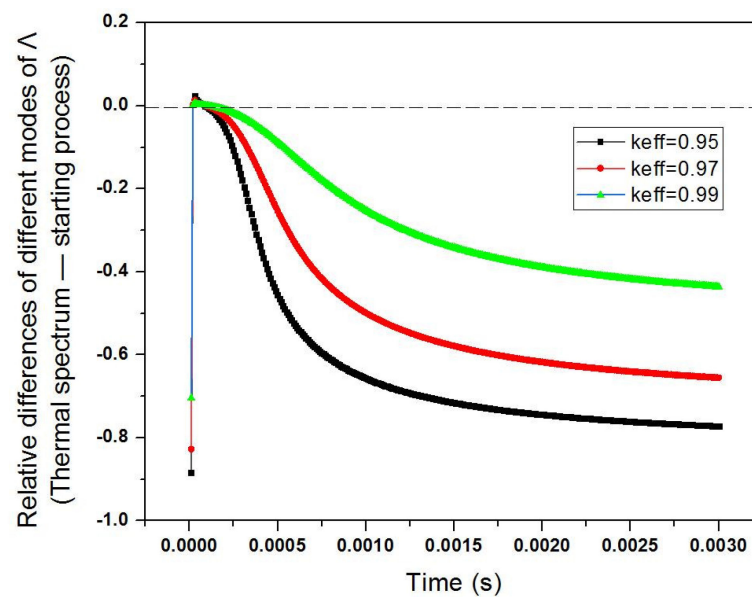


**Figure 10.** Relative differences in  $\Lambda$  with time for different modes of the thermal spectrum, under different subcriticalities and starting processes.

It can be seen from Figure 9 that the relative difference in  $\Lambda$  between both the modes decreases sharply at the start and becomes smooth as the time increases under the beam trip scenario. Figure 10 shows that the relative  $\Lambda$  differences between the two modes fluctuate largely at the beginning of starting process and increase gradually with the increase in time. In both cases the relative difference  $\Lambda$  between both modes increases with the deepening of the subcriticality.

The relative differences in  $\beta_{\text{eff}}$  with time for the  $\lambda$  and  $\alpha$  modes are shown in Figures 11 and 12 for the beam trip and starting process, respectively.

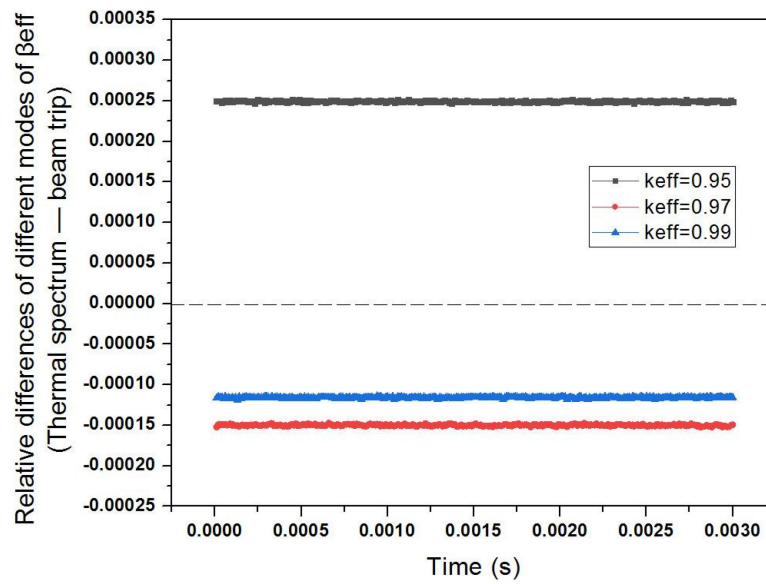


**Figure 11.** Relative differences in  $\beta_{eff}$  with time for different modes of the thermal spectrum, under different subcriticalities and beam trips.

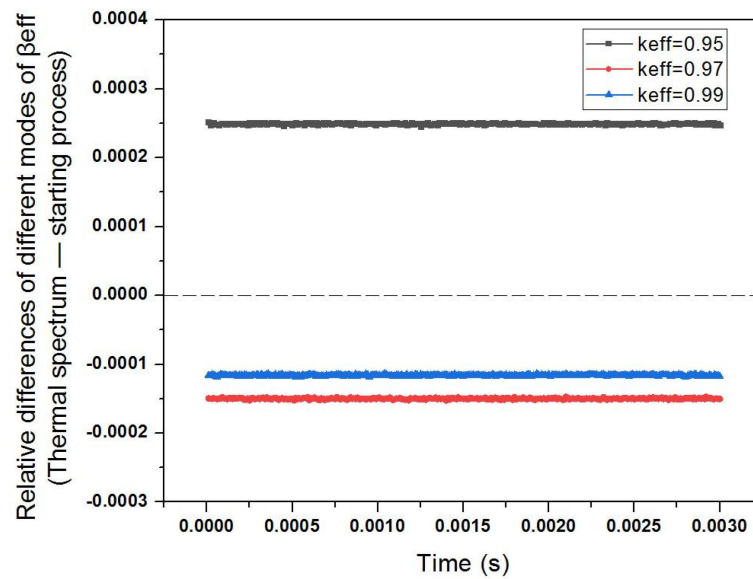


**Figure 12.** Relative differences in  $\beta_{eff}$  with time for different modes of the thermal spectrum, under different subcriticalities and starting processes.

From Figure 11, the relative differences in  $\beta_{eff}$  between the two modes tend to be smooth under beam trip and increase with the deepening of the subcriticality. Figure 12 shows that the relative differences in  $\beta_{eff}$  between the two modes tend to be smooth under the starting process and increase with the deepening of the subcriticality.

#### 4.3. Analysis of Physical Mechanism

Comparing the results in Sections 4.1 and 4.2, it can be seen that for the kinetic parameters ( $\Lambda$  and  $\beta_{eff}$ ) of an ADSR with a fast spectrum and thermal spectrum, the trends of the relative differences in the kinetic parameters of the  $\lambda$  and  $\alpha$  modes are basically the same under the beam trip and starting process. The relative differences in the kinetic parameters of the two modes both increase with the increase in the subcriticality. For different beam transients, the size of the relative variances in the kinetic parameters of the ADSR between the fast and thermal spectra varies. This is mostly because the thermal

spectrum in the thermal neutron zone is substantially higher than the fast spectrum, and the overall difference between the spectra is large.

For the study of  $\Lambda$ , at the start of the beam transients, the rapid decrease or increase in the external source leads to a sharp fluctuation in the neutron fluence rate distribution in time and space for the whole ADSR, which makes a large fluctuation in  $\Lambda$ . As the ADS progressively stabilizes, so does the neutron fluence rate distribution of the ADSR, causing it to stabilize  $\Lambda$ . The influence of the external source becomes more obvious as the subcritical state develops, resulting in a high heterogeneity of neutron fluence rate in time–space, which increases the relative difference between both modes. The influence of external sources becomes increasingly apparent in the analysis of  $\beta_{\text{eff}}$  as subcriticality grows, and the difference in neutron fluence rate distribution increases for different modes, leading to an increase in the relative difference of  $\beta_{\text{eff}}$  for different modes.

For the beam transients without beam current, such as the beam trip, the process from the presence to the absence of the spallation neutron source leads to the dramatic change in the neutron breeding characteristics of the ADS and the complex time–space evolution behavior of the neutron fluence rate. This process is proposed to be described by the homogenized group constants of the  $\alpha$  eigenvalue mode [17].

For the beam transients with beam current, such as the starting process, the beam transient changes the intensity of the spallation neutron source, and the neutron breeding characteristics of the ADS remain unchanged. The neutron fluence rate is not significantly different from that of the steady-state spallation neutron source drive. This process is recommended to be described by the homogenized group constants of the steady-state external source drive mode [17]. Because the physical mechanism of the  $\lambda$  eigenvalue mode is comparable to that of the steady-state external source-driven mode, by modifying the generation source term, they both cause the reactor to reach virtual criticality, and the difference in generating the homogenized group constants is negligible [20]. Thus, the  $\lambda$ -mode homogenized group constants are also suitable for the beam transients with beam current.

The MC homogenization method for ADSR time–space neutron kinetics can be constructed by linking the MC-homogenized group constants for  $\lambda$  mode and  $\alpha$  mode and adapting them to the beam current and without beam current conditions, respectively. This approach is based on the authors' prior multi-mode core few-group constants method, and it directly employs the MC method to generate distinct modes of homogenized group constants [18–20]. It will be more adaptable to the physical features of the ADSR during beam transients than earlier techniques and will provide a more accurate description of the subcriticality and high heterogeneity of neutron fluence rate in time–space.

## 5. Conclusions

In this study, we investigated the influence mechanism of neutron time–space kinetics in an ADSR under different neutron spectra, subcriticalities, and beam transients. The MC homogenization method for ADSR time–space neutron kinetics is developed. The effects of the deep subcriticality and the high heterogeneity of neutron fluence rate in time–space of the ADSR on its kinetics parameters are clarified. The following conclusions can be derived from the findings presented in this study.

(1) The computational accuracy of the MC homogenization method with  $\alpha$  eigenvalue mode is higher than that of the MC homogenization method with  $\lambda$  eigenvalue mode under various subcriticalities. Thus, the MC homogenization method with  $\alpha$  eigenvalue mode is more adaptable to the subcriticality characteristics.

(2) Under the beam transient condition, the relative differences in the kinetic parameters ( $\Lambda$  and  $\beta_{\text{eff}}$ ) of the ADSR for different modes of the fast/thermal neutron spectra are incremented with the deepening of the subcriticality, and the differences in  $\Lambda$  are larger than those of  $\beta_{\text{eff}}$  for varied modes. The impact of deep subcriticality and the great heterogeneity of neutron fluence rate in time–space on the mechanism of neutron time–space kinetics of ADSR during beam transients should be considered.

(3) For the study of neutron time–space kinetics in ADSR, it is recommended to adopt a more adaptable MC homogenization method for ADSR time–space neutron kinetics.

**Author Contributions:** Conceptualization, N.D. and C.X.; methodology, N.D. and C.H.; software, C.X. and Z.L.; validation, J.X. and C.H.; formal analysis, N.D.; investigation, C.X.; resources, Z.L.; data curation, N.D.; writing—original draft preparation, N.D.; writing—review and editing, N.D. and C.H.; visualization, J.X.; supervision, J.X. and T.Y.; project administration, J.X. and T.Y.; funding acquisition, J.X. and T.Y. All authors have read and agreed to the published version of the manuscript.

**Funding:** This work is supported by the National Natural Science Foundation of China (No. U2267207 and No. 11875162), Project of Hunan Provincial Education Department (No. 21C0271), University-level research project of University of South China (No. 210XQD029), and Science and Technology innovation Program of Hunan Province (No. 2020RC4053).

**Data Availability Statement:** Not applicable.

**Acknowledgments:** We thank all the teachers in the NEAL group of the School of Nuclear Science and Technology of USC for their guidance and the students for their help.

**Conflicts of Interest:** The authors declare no conflict of interest.

## References

- Zhan, W.; Yang, L.; Yan, X.; Zhang, X. Accelerator-driven advanced nuclear energy system and its research progress. *At. Energy Sci. Technol.* **2019**, *53*, 1809.
- Li, R.; Li, L.; Wang, Q. The impact of energy efficiency on carbon emissions: Evidence from the transportation sector in Chinese 30 provinces. *Sustain. Cities Soc.* **2022**, *82*, 103880. [[CrossRef](#)]
- Zhang, Q. Recommendations of accelerate the development of nuclear power plant spent fuel reprocessing. *Energy China* **2019**, *41*, 44–47.
- Zhan, W.L.; Xu, H.S. Advanced fission energy program-ADS transmutation system. *Bull. Chin. Acad. Sci.* **2012**, *27*, 375–381.
- Zhao, Z.; Xia, H. Study on ADS and the sustainable development of nuclear energy. *China Nucl. Power* **2009**, *2*, 202–211. [[CrossRef](#)]
- Ahmad, A.; Lindley, B.A.; Parks, G.T. Accelerator-induced transients in accelerator driven subcritical reactors. *Nucl. Instrum. Methods Phys. Res. Sect. A* **2012**, *696*, 55–65. [[CrossRef](#)]
- Shen, F.; Wang, S. Point kinetic equation of ADS sub-critical reactor. *At. Energy Sci. Technol.* **2011**, *45*, 1300.
- Zhang, L. Studies on the Typical Kinetic Process of Fast and Thermal Lead Reactor the Venus-II. Ph.D. Thesis, Institute of Modern Physics, Chinese Academy of Sciences, Beijing, China, 2018.
- Wu, G. Research on Continuous Energy Monte Carlo Homogenization and Group Constant Generation Based on RMC. Ph.D. Thesis, Tsinghua University, Beijing, China, 2018.
- Li, Y. Research on Homogenization with Discrete Angel Based on Monte Carlo Method. Ph.D. Thesis, Tsinghua University, Beijing, China, 2018.
- Talamo, A.; Gohar, Y.; Kiyavitskaya, H.; Bournos, V.; Fokov, Y.; Routkovskaya, C. Monte Carlo and deterministic neutronics analyses of YALINA thermal facility and comparison with experimental results. *Nucl. Technol.* **2013**, *184*, 131–147. [[CrossRef](#)]
- Talamo, A.; Gohar, Y.; Aliberti, G.; Cao, Y.; Smith, D.; Zhong, Z.; Serafimovich, I. MCNPX, MONK, and ERANOS analyses of the YALINA Booster subcritical assembly. *Nucl. Eng. Des.* **2011**, *241*, 1606–1615. [[CrossRef](#)]
- He, M.; Wu, H.; Zheng, Y.; Wang, K.; Li, X.; Zhou, S. Beam transient analyses of Accelerator Driven Subcritical Reactors based on neutron transport method. *Nucl. Eng. Des.* **2015**, *295*, 489–499. [[CrossRef](#)]
- Picca, P.; Rurfaro, F. Multi-generation point kinetics for subcritical systems. *Ann. Nucl. Energy* **2021**, *162*, 108527. [[CrossRef](#)]
- Wang, S.; Shen, F. Adjoint equation of ADS sub-critical reactor. *At. Energy Sci. Technol.* **2011**, *45*, 775.
- Stanisz, P.; Oettingen, M.; Cetnar, J. Development of a trajectory period folding method for burnup calculations. *Energies* **2022**, *15*, 2245. [[CrossRef](#)]
- Yu, T.; Xie, J.; Liu, J. Analysis method of dynamic characteristics of subcritical reactor of ADS induced by accelerator beam transients. *Nucl. Power Eng.* **2014**, *35*, 48–51.
- Deng, N. Research on the Space-Time Kinetics of ADS Subcritical Reactor under Beam Transients Based on Multi-Mode Few-Group Constant Library. Ph.D. Thesis, University of South China, Hengyang, China, 2021.
- Deng, N.; Xie, J.; Hou, C.; Zeng, W.; Chen, Z.; Yu, T.; Xie, Q. Dynamic Characteristics of Accelerator-Driven Subcritical Reactor With Self-Adapting Multi-Mode Core Few-Group Constants. *Front. Energy Res.* **2021**, *8*, 603084. [[CrossRef](#)]
- Deng, N.B.; Ding, D.X.; Xie, J.S.; Yu, T.; Hou, C. The Influence Mechanism of Space-Time Kinetics of ADS Subcritical Reactor under Beam Transients. *Int. J. Energy Res.* **2023**, *2023*, 1775438. [[CrossRef](#)]
- Wu, G.C.; Wang, G.B.; Wang, K.; Yu, G.L. Core Physics Analysis of Plate-fuel Research Reactor Introducing Neutron Trap Structure Based on MC Method. *At. Energy Sci. Technol.* **2015**, *49*, 81.
- ZHOU, S.C.; WU, H.C.; CAO, L.Z.; ZHENG, Y.Q. Development of neutronics analysis code system for accelerator driven subcritical reactor. *At. Energy Sci. Technol.* **2013**, *47*, 458.

23. Romano, P.K.; Horelik, N.E.; Herman, B.R.; Nelson, A.G.; Forget, B.; Smith, K. OpenMC: A state-of-the-art Monte Carlo code for research and development. *Ann. Nucl. Energy* **2015**, *82*, 90–97. [[CrossRef](#)]
24. Variansyah, I.; Betzler, B.R.; Martin, W.R. Multigroup Constant Calculation with Static  $\alpha$ -Eigenvalue Monte Carlo for Time-Dependent Neutron Transport Simulations. *Nucl. Sci. Eng.* **2020**, *194*, 1025–1043. [[CrossRef](#)]
25. Kia, H.A.; Zangian, M.; Minuchehr, A.; Zolfaghari, A.R. Implementation and comparison of different prompt and delayed  $\alpha$ -static approaches. *Prog. Nucl. Energy* **2019**, *114*, 210–226. [[CrossRef](#)]
26. Li, Z.; Xie, J.; Xu, S.; Deng, N.; Yuan, X.; Yu, T. Development and Verification of Calculation Module for Prompt Neutron Attenuation Constant Based on OpenMC. *At. Energy Sci. Technol.* **2022**, *56*, 1906–1914.
27. Cao, Y. Space-Time Kinetics and Time-Eigenfunctions. Ph.D. Thesis, University of Michigan, Ann Arbor, MI, USA, 2008.
28. Hou, C.; Yu, T.; Xie, J. The effects of the shape function and weighting function on the kinetics of the ADS sub-critical reactor. *Nucl. Tech.* **2018**, *41*, 77–86.
29. Rimpault, G.; Plisson, D.; Tommasi, J.; Jacqmin, R.; Rieunier, J.M.; Verrier, D.; Biron, D. The ERANOS code and data system for fast reactor neutronic analyses. In Proceedings of the PHYSOR 2002-International Conference on the New Frontiers of Nuclear Technology: Reactor Physics, Safety and High-Performance Computing, Seoul, Republic of Korea, 7–10 October 2002.

**Disclaimer/Publisher’s Note:** The statements, opinions and data contained in all publications are solely those of the individual author(s) and contributor(s) and not of MDPI and/or the editor(s). MDPI and/or the editor(s) disclaim responsibility for any injury to people or property resulting from any ideas, methods, instructions or products referred to in the content.